Journal of Solid State Chemistry 182 (2009) 730–735

Contents lists available at ScienceDirect

Journal of Solid State Chemistry

journal homepage: www.elsevier.com/locate/jssc

Structural investigation of Eu^{2+} emissions from alkaline earth zirconium phosphate

Masaaki Hirayama [a], Noriyuki Sonoyama [b], Atsuo Yamada [a], Ryoji Kanno [a,*]

[a] Department of Electronic Chemistry, Interdisciplinary Graduate School of Science and Engineering, Tokyo Institute of Technology, 4259 Nagatuta, Midori-ku, Yokohama 226-8502, Japan

[b] Graduate School of Engineering, Environmental Technology and Urban Planning, Nagoya Institute of Technology, Gokiso-cho, Showa-ku, Nagoya 466-8555, Japan

ARTICLE INFO

Article history:
Received 23 August 2008
Received in revised form
7 December 2008
Accepted 9 December 2008
Available online 30 December 2008

Keywords:
Phosphor
NASICON
Spectroscopy
Rietveld analysis

ABSTRACT

Eu^{2+} doped $A_{0.5}Zr_2(PO_4)_3$ (A = Ca, Sr, Ba) phosphors with the NASICON structure were synthesized by a co-precipitation method. Their photoluminescent and structural properties were investigated by photoluminescent spectroscopy and powder X-ray Rietveld analysis, which determined two sites for Eu^{2+} ions in the host structure, 3*a* and 3*b*. The Eu–O bond lengths were increased by changing alkaline earth ions from Ca to Ba, causing Eu^{2+} emission bands to shift from blue-green to blue. A correlation was observed between the peak wavelength positions and the Eu–O bond length. The photoluminescent properties are discussed in terms of crystal field strength and nephelauxetic effect, and a schematic diagram of Eu^{2+} emissions is proposed for the Eu^{2+} doped NASICON phosphor.

1. Introduction

Much recent attention has been paid to phosphors suitable for light-emitting diode (LED) based solid-state lighting. White LEDs offer the advantages of high brightness, low power consumption, and longer lifetime compared to conventional light bulbs and fluorescent lamps [1,2]. The most common approach involves combining a blue GaInN LED chip (460 nm) with a yellow-emitting phosphor, $Y_3Al_5O_{12}:Ce^{3+}$. This system has a low color-rendering index because of its deficiency in the red region of the visible spectrum. One approach to overcome this drawback is to add a red-emitting phosphor to compensate for the deficiency [3–5]. Another approach is to develop a new white LED system consisting of ultraviolet (UV) LEDs (300–410 nm) with red, blue, and green phosphors [6–8]. This system is suitable for white LEDs with an excellent color-rendering index and high color tolerance. To advance this technology, phosphors with desirable color emission and high efficiency under UV excitation must be developed.

Eu^{2+} doped alkaline metal phosphates are one class of desirable phosphors for UV excitation [9]. In this work, we focused on phosphates with the NASICON (sodium silicon conductor) structure, which consists of a three-dimensional network of MO_6 (M = Ti, Zr, Hf) octahedra, sharing corners with PO_4 tetrahedra and containing interstitial A ions (A = alkaline or alkaline earth metal) [10] (Fig. 1). Phosphate NASICONs could offer several conditions suitable for Eu^{2+} doped phosphor: (i) The covalent $M_2(PO_4)_3$ framework has high thermal stability. (ii) Eu^{2+} is expected to substitute for A ion sites, which are separated from each others by distances >5 Å [11,12]. The location would inhibit concentration quenching of Eu^{2+} emission intensity. (iii) Crystal field strength and covalency of the Eu–O bond, which are related to the energy of the $4f^6 5d^1$ level in Eu^{2+}, could be easily controlled by changing the chemical composition of the NASICON structure [13–16]. Although NASICON compounds have attracted significant attention for their diversity of fast-ionic conductivity [16,17] and low thermal expansion [18,19], as well as the dependence of these properties on the framework structure, few studies have focused on their photoluminescent properties. Even though NASICON-type $Eu^{II}_{0.5}Zr_2(PO_4)_3$ has been reported to be an efficient blue phosphor [20], the luminescent characteristics have not been investigated in detail. In the present study, we synthesized Eu^{2+} doped $A_{0.5}Zr_2(PO_4)_3$ (A = Ca, Sr, Ba), and demonstrated continuous changes in emission wavelengths of Eu^{2+} by alkaline earth ions. The locations of Eu^{2+} were determined by X-ray Rietveld structural analysis, and effects of the framework structural changes on luminescent properties were discussed in terms of crystal field strength and covalency of the Eu–O bond.

2. Experimental section

Eu^{2+} doped $A_{0.5}Zr_2(PO_4)_3$ (A = Ca, Sr, Ba) were synthesized by the co-precipitation method previously reported by Orlova et al.

* Corresponding author. Fax: +81 45 924 5401.
E-mail address: kanno@echem.titech.ac.jp (R. Kanno).

0022-4596/$ - see front matter © 2008 Elsevier Inc. All rights reserved.
doi:10.1016/j.jssc.2008.12.015

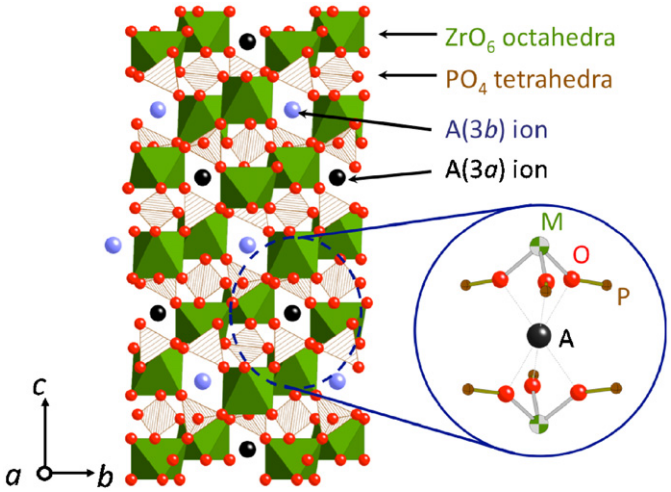

Fig. 1. Structure of NASICON phosphates, $A_{0.5}Zr_2(PO_4)_3$ (A = Ca, Sr, Ba). A ions are located at interstitial cavities in the $Zr_2(PO_4)_3$ framework structure consisting of the Zr–O and P–O covalent bonds.

[21]. Stoichiometric proportions of $Ca(NO_3)_2 \cdot 7H_2O$ (Wako, 99%), $Sr(NO_3)_2$ (High Purity Chemicals Lab., 99%), $Ba(NO_3)_2$ (Wako, 99.0%), $ZrO(NO_3)_2 \cdot 2H_2O$ (Kanto Chemical, >99.0%), and $Eu(NO_3)_3 \cdot 6H_2O$ (Kanto Chemical Co., 99.95%) were dissolved in distilled water. The addition of a solution of 0.1 M H_3PO_4 (Wako, 99.9%) in appropriate proportion, under constant stirring, produced a colorless gel. After evaporation of the solution, the sol was successively calcined at 500 and 800 °C for 12 h. The powders were sintered at 1000 °C for 12 h under 2%-H_2/Ar gas. Powder X-ray diffraction (XRD) patterns were obtained using an X-ray diffractometer (Rigaku RU-200B) with 12 kW Cu$K\alpha$ radiation, and collected at 0.03° step widths over a 2θ range from 10° to 120°. The structural and profile parameters were refined by Rietveld analysis, using the refinement program RIETAN2000 [22]. The structural parameters of $A_{0.5}Zr_2(PO_4)_3$:Eu^{2+} were refined with an R-3 space group using the following structural model (using Wyckoff notation): A and Eu at 3a and 3b sites, Zr at 6c sites, and P and O at 18f sites. A virtual chemical specie, M, which consisted of A and Eu with the composition ratio, was introduced to refine the distribution of the site occupancy among 3a and 3b sites, because it was rather difficult to refine the distribution of Eu^{2+} among these sites independently of alkaline earth ions because of a small volume of Eu. The XRD patterns with impurity phases were refined with multi-phase models. The excitation and emission spectra in the UV to visible region were obtained by a fluorophotometer (SPEX Fluoromax) at room temperature using a xenon lamp excitation source.

3. Results and discussion

3.1. Characterization

Fig. 2 shows the XRD patterns for $A_{0.5}Zr_2(PO_4)_3$:0.01Eu^{2+} (A = Ca, Sr, Ba). The diffraction peaks can be assigned to the NASICON structure with the R-3 space group [23,24]. The peaks shifted to lower degrees from Ca to Ba systems, resulting from the lattice expansion. Several samples also contained a small amount of ZrP_2O_7 phase (Pm-3). To evaluate the impurity effect, we synthesized ZrP_2O_7 and ZrP_2O_7:Eu under the same conditions as $A_{0.5}Zr_2(PO_4)_3$:Eu^{2+}. No significant difference in the cell parameter was observed between Eu^{2+} doped ZrP_2O_7 (8.2635(5) Å) and undoped ZrP_2O_7 (8.2640(7) Å). A very weak peak around 460 nm of Eu^{2+} in EuO [25] was observed in the photoluminescence (PL)

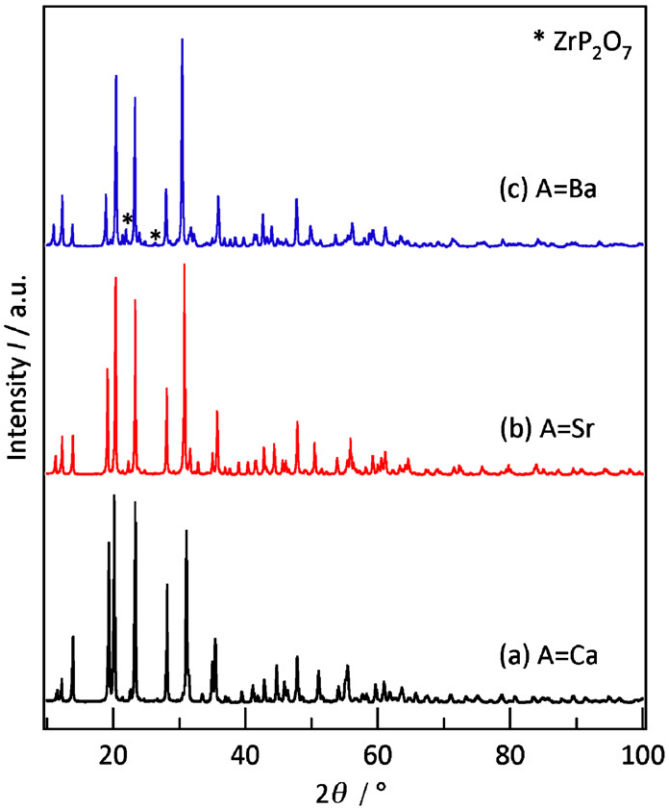

Fig. 2. Powder X-ray diffraction patterns of $A_{0.5}Zr_2(PO_4)_3$:0.01Eu^{2+} (M = Ca, Sr, Ba).

spectra of ZrP_2O_7:Eu, while no emission of Eu^{3+} in ZrP_2O_7 [26] and Eu_2O_3 [27] was observed. These results indicates that ZrP_2O_7:Eu constituted of pure ZrP_2O_7 and EuO phases.

Fig. 3 shows PL excitation (PLE) and PL spectra of $A_{0.5}Zr_2(PO_4)_3$:0.01Eu^{2+}. The main excitation peaks extended from 300 to 400 nm, indicating that the phosphors are suitable for near-UV excitation. The phosphors exhibited broad emissions around 400–600 nm, corresponding to transitions between the crystal field components of the $4f^6 5d^1$ excited state and the $4f^7$ ground state in Eu^{2+}. After changing alkaline earth ions from Ca to Ba, peak wavelengths shift from 484.4 to 435.0 nm with a decrease in full-width at half-maximum (FWHM) values. Fig. 4 shows the PL spectra of $(Ca_{1-x}Eu_x)_{0.5}Zr_2(PO_4)_3$ at different Eu concentrations (x = 0.005–0.10). The positions of the emission peaks showed blue-shift behavior with increasing Eu concentrations. These results demonstrate that the chromaticity of the Eu^{2+} doped NASICON phosphors change with the A cation species. The emission intensity increased continuously with increasing Eu concentration, and no concentration quenching was observed until x = 0.10.

3.2. Structural investigations

The location of Eu^{2+} in the NASICON structure was investigated by the structural analysis for $Ca_{0.5}Zr_2(PO_4)_3$:Eu^{2+} varying Eu concentrations. Fig. 5 shows the dependence of lattice parameter on Eu concentration for $(Ca_{1-x}Eu_x)_{0.5}Zr_2(PO_4)_3$ (x = 0, 0.01, 0.05, 0.10). The a parameter decreased and the c parameter increased with increasing Eu concentration, following Vegard's law. This indicates the incorporation of Eu^{2+} ions into the NASICON structure. Pet'kov et al. have investigated lattice changes in NASICON-type $A'_{0.5}Zr_2(PO_4)_3$ (A' = Cd, Ca, Sr, Ba) [28]. The parameter a decreased and the parameter c increased with increasing radius of A' cations, which occupy half of the interstitial

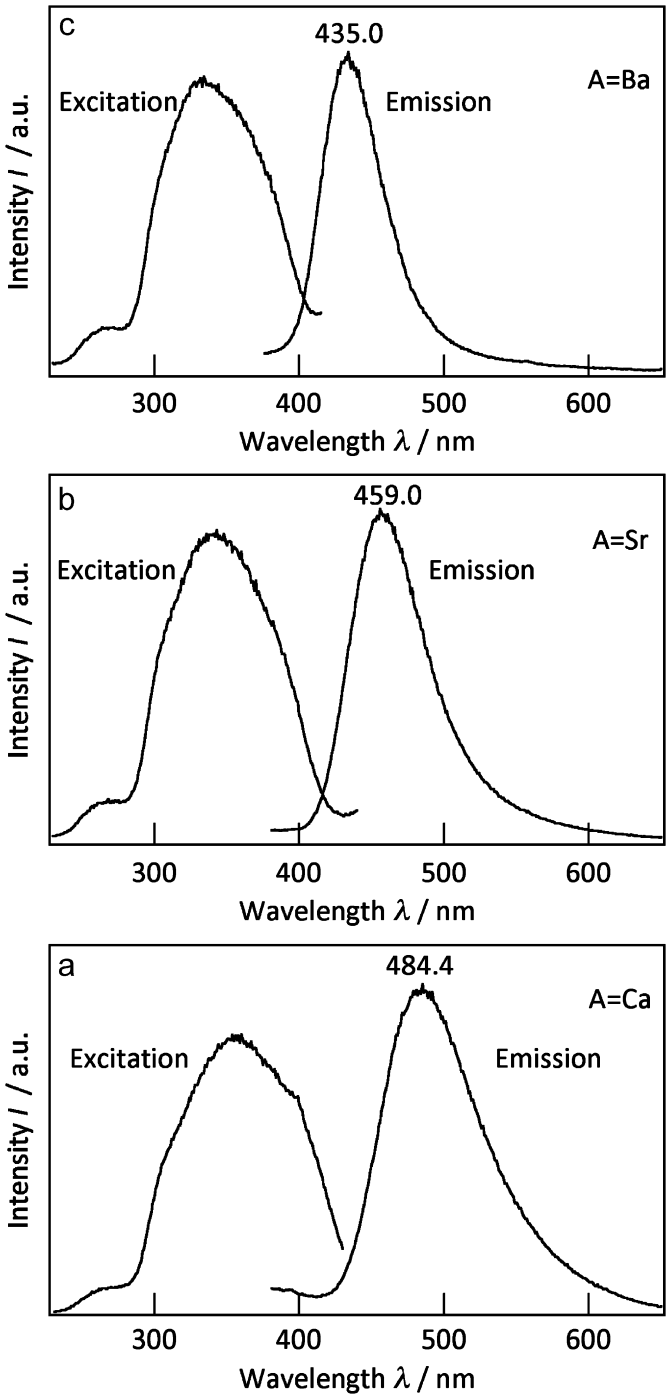

Fig. 3. Excitation (left) and emission (right) spectra of the luminescence of $A_{0.5}Zr_2(PO_4)_3$:0.01Eu^{2+} at room temperature, (a) A = Ca, (b) A = Sr, (c) A = Ba. The excitation spectra were recorded for 486, 456, and 434 nm, respectively, and the emission spectra were recorded for 350, 341, and 335 nm, respectively. The excitation spectra are not corrected for the Xenon lamp intensity.

cavities situated between neighboring ZrO_6 octahedra along the c axis. The lattice changes of $(Ca_{1-x}Eu_x)_{0.5}Zr_2(PO_4)_3$ with increasing Eu concentration indicated the substitution of Eu^{2+} for interstitial Ca^{2+}, because Eu^{2+} has larger ion radii (1.2 Å) than Ca^{2+} ion (1.0 Å) [29]. Therefore, the structure of $Ca_{0.5}Zr_2(PO_4)_3$ was used as a starting structural model for the Rietveld analysis.

Fig. 6a shows a typical Rietveld result for $(Ca_{1-x}Eu_x)_{0.5}Zr_2(PO_4)_3$ ($x = 0.10$). The refined parameters are summarized in

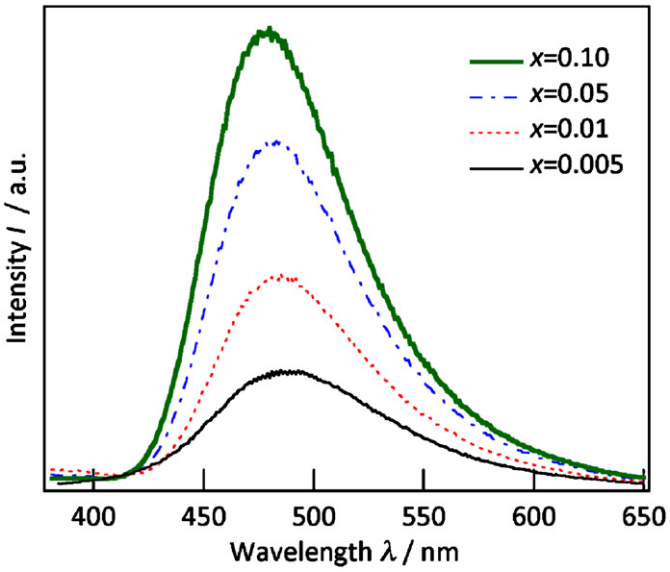

Fig. 4. Emission spectra of the luminescence of $(Ca_{1-x}Eu_x)_{0.5}Zr_2(PO_4)_3$ with varying amount of Eu^{2+} ($x = 0.005$, 0.01, 0.05, 0.1). The spectra were recorded for 350 nm.

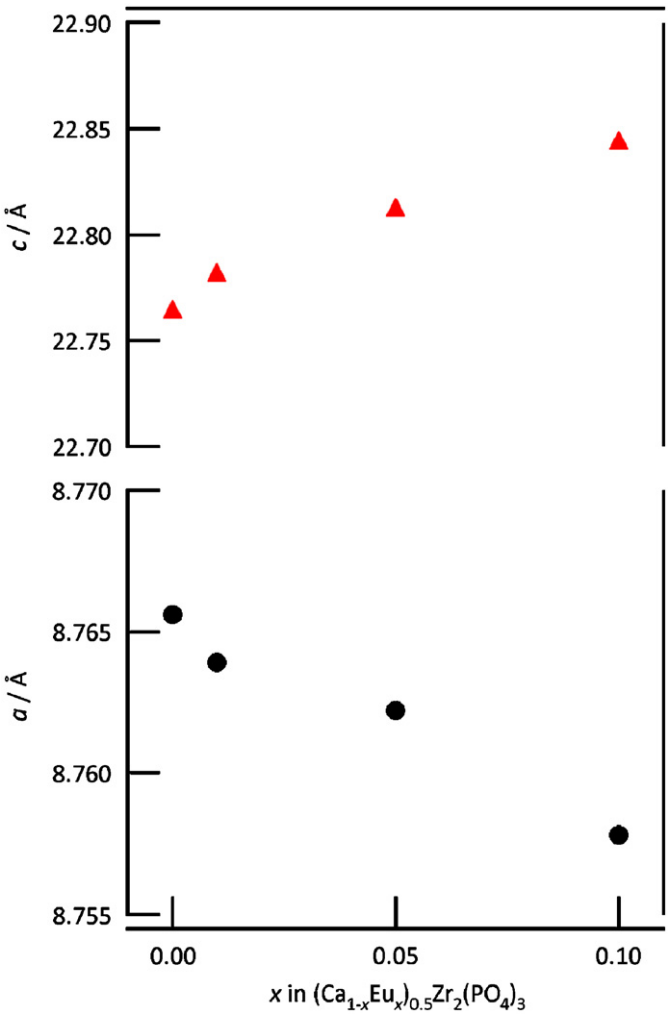

Fig. 5. Cell parameter dependences on Eu concentration in $(Ca_{1-x}Eu_x)_{0.5}Zr_2(PO_4)_3$.

Table 1. The Ca and Eu ions occupy both 3*a* and 3*b* sites, with a distribution of 89.6% and 10.4%, respectively. No significant change in the distribution of 3*a* and 3*b* sites was observed with changing Eu concentration. These sites are located in the elongated antiprism formed by the triangular faces of two ZrO_6 octahedra, and therefore have a similar local environment. No peak separation of Eu^{2+} emissions from each site in the PL spectra seems to be related to the Eu distribution and the similarity of the site environment among 3*a* and 3*b* sites. Fig. 6b and c show Rietveld results for $(Sr_{0.99}Eu_{0.01})_{0.5}Zr_2(PO_4)_3$ and $(Ba_{0.99}Eu_{0.01})_{0.5}Zr_2(PO_4)_3$, which were refined using the same structural model as was used for $(Ca_{1-x}Eu_x)_{0.5}Zr_2(PO_4)_3$. Eu ions substituted for Sr^{2+} (1.2 Å) and Ba^{2+} (1.3 Å) ions, which both have larger ionic radii than Ca^{2+} ions (1.0 Å). Table 2 summarizes the lattice parameters, Eu–O bond lengths, and peak energies of Eu^{2+} emissions for $(A_{1-x}Eu_x)_{0.5}Zr_2(PO_4)_3$ (A = Ca, Sr, Ba; x = 0–0.1). The lengths of the Eu–O bond, which is almost parallel to the *c* axis (Fig. 1), increased with lattice expansion along the *c* axis. The long distance between neighboring Eu^{2+} ions (over 6 Å) may enable high concentration-quenching performance of Eu^{2+}-doped NASICON phosphors.

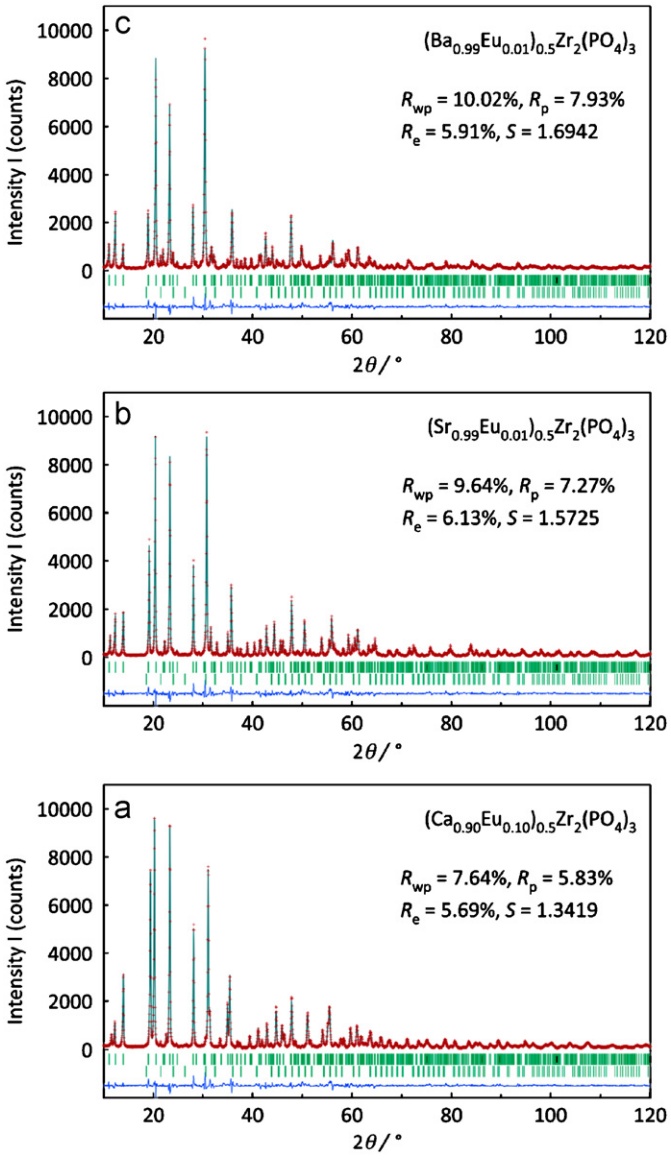

Fig. 6. X-ray Rietveld result of $(Ca_{0.90}Eu_{0.10})_{0.5}Zr_2(PO_4)_3$, $(Sr_{0.99}Eu_{0.01})_{0.5}Zr_2(PO_4)_3$, and $(Ba_{0.99}Eu_{0.01})_{0.5}Zr_2(PO_4)_3$. The observed intensity data are shown by dots, and the solid line overlying them is the calculated intensity. Vertical markers below the diffraction patterns indicate positions of possible Bragg reflections. Differences between the observed and calculated intensities are plotted as D_{yi} at the bottom in the same scale.

Table 1
Rietveld refinement results for $Ca_{0.5}Zr_2(PO_4)_3$:0.10Eu^{2+}.

Atom	Site	g	x	y	z	B_{eq}/Å^2
Phase 1 $(Ca_{0.90}Eu_{0.10})_{0.5}Zr_2(PO_4)_3$						
M(1)	3*a*	0.896 (8)	0	0	0	1.8 (11)
M(2)	3*b*	= 1−*g*(*M*(1))	0	0	0.5	= *B*(M(1))
Zr(1)	6*c*	1	0	0	0.14895(8)	0.50 (2)
Zr(2)	6*c*	1	0	0	0.64111 (8)	= *B*(Zr(1))
P(1)	18*f*	1	0.2914 (5)	0.0094 (8)	0.2527 (2)	1.12 (7)
O(1)	18*f*	1	0.188 (10)	0.009 (10)	0.1932 (4)	1.10 (8)
O(2)	18*f*	1	0.054 (10)	−0.162 (10)	0.6956 (3)	= *B*(O(1))
O(3)	18*f*	1	0.1808 (9)	0.1713 (8)	0.0832 (3)	= *B*(O(1))
O(4)	18*f*	1	0.8359 (9)	0.7913 (9)	0.5948 (3)	= *B*(O(1))
Phase 2 ZrP_2O_7						
Zr(3)	4*a*	1	0	0	0	0.6
P(2)	8*c*	1	0.3926 (9)	= *x*(P(2))	= *x*(P(2))	1
O(5)	24*d*	1	0.481 (13)	0.225 (9)	0.423 (2)	1
O(6)	4*b*	1	1/2	1/2	1/2	1

Space group $R\bar{3}$, a = 8.7585 (2) Å, c = 22.8431(4) Å, R_I = 2.36, R_F = 1.02.
Space group $Pa\bar{3}$, a = 8.261 (3) Å, R_I = 2.73, R_F = 1.12.
R_{wp} = 7.64%, R_p = 5.83%, R_e = 5.69%, $S = R_{wp}/R_e$ = 1.3419.
Mass fraction phase1: phase2 = 0.992: 0.008.

3.3. *Effects of local structure on luminescent properties*

Eu^{2+} ions exhibit broadband emissions, which are attributed to the transition from the $4f^65d^1$ excited state to the $4f^7$ ground state. The energy level of the external 5*d* orbital depends on the host structure, changing the wavelength of the emission bands from near-UV to red [13]. The effects of the host structure have been explained as arising mainly from two factors, crystal field effect and nephelauxetic effect [13–16].

Our Rietveld analysis of $A_{0.5}Zr_2(PO_4)_3$ (A = Ca, Sr, Ba) confirmed that the Eu ion occupies interstitial 3*a* and 3*b* sites in the covalent $Zr_2(PO_4)_3$ framework: Eu ions located in relatively ionic environments and created the ionic bonds with ligand oxygen. Therefore, the lowest $4f^65d^1$ state of Eu^{2+} depends is related to the crystal field strength. In the case that Eu^{2+} ions have similar bond character to the ligand O^{2-} ions, the crystal field splitting becomes larger with decreasing Eu–O bond length [15], leading to a decrease in the difference between the 4*f* and 5*d* energy levels in Eu^{2+}. The emission bands of Eu^{2+} shift to a higher energy with an increase in crystal field strength. Table 2 summarizes the relationship between the energies of the 4*f*–5*d* transition in Eu^{2+} and the Eu–O bond lengths in $(A_{1-x}Eu_x)_{0.5}Zr_2(PO_4)_3$ (A = Ca, Sr, Ba). A clear correlation was experimentally observed between the energies of Eu^{2+} emissions and the Eu–O bond length. Matsui et al. reported luminescent properties of $Eu_{0.5}Zr_2(PO_4)_3$ with the NASICON structure [19]. $Eu_{0.5}Zr_2(PO_4)_3$ has lattice parameters similar to $Sr_{0.5}Zr_2(PO_4)_3$ due to the very similar ion radii of Eu^{2+} and Sr^{2+}. The peak wavelength of $Eu_{0.5}Zr_2(PO_4)_3$ was appeared around 460 nm, which is very similar to that of $(Sr_{0.99}Eu_{0.01})_{0.5}Zr_2(PO_4)_3$ (459.0 nm) shown in the present study. This result indicated that the Eu–O bond length is a key parameter of emission energies of Eu^{2+} in $A_{0.5}Zr_2(PO_4)_3$ (A = Ca, Sr, Ba). Fig. 7 shows a schematic energy level diagram of Eu^{2+} ions in $A_{0.5}Zr_2(PO_4)_3$ NASICONs as a function of crystal field strength. These results demonstrate that chromaticity of Eu^{2+} emissions in the NASICON structure are controlled by changing the Eu–O bond length.

Table 2
Lattice parameters, Eu–O bond lengths, and Eu^{2+} emission energies of $(A_{1-x}Eu_x)_{0.5}Zr_2(PO_4)_3$ (A = Ca, Sr, Ba).

	a/Å	c/Å	Eu(3a)–O d/Å	Eu(3b)–O d/Å	Peak energy of Eu^{2+} emission E/eV
$Ca_{0.5}Zr_2(PO_4)_3$	8.7956(2)	22.6831(3)	2.445(2)	2.725(3)	–
$(Ca_{0.99}Eu_{0.01})_{0.5}Zr_2(PO_4)_3$	8.7743(6)	22.7851(11)	2.445(7)	2.731(8)	2.559
$(Ca_{0.95}Eu_{0.05})_{0.5}Zr_2(PO_4)_3$	8.7622(4)	22.8112(7)	2.450(7)	2.735(8)	2.569
$(Ca_{0.90}Eu_{0.10})_{0.5}Zr_2(PO_4)_3$	8.7578(3)	22.8429(5)	2.451(2)	2.733(8)	2.583
$(Sr_{0.99}Eu_{0.01})_{0.5}Zr_2(PO_4)_3$	8.6947(5)	23.3821(10)	2.535(7)	2.829(8)	2.701
$(Ba_{0.99}Eu_{0.01})_{0.5}Zr_2(PO_4)_3$	8.659(10)	23.9241(2)	2.734(8)	2.888(12)	2.850

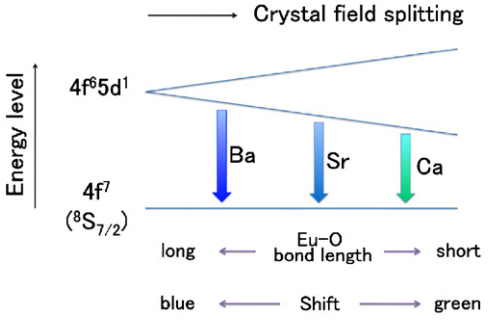

Fig. 7. Schematic energy level diagram of Eu^{2+} ions in the $A_{0.5}Zr_2(PO_4)_3$ NASICONs as a function of the crystal field.

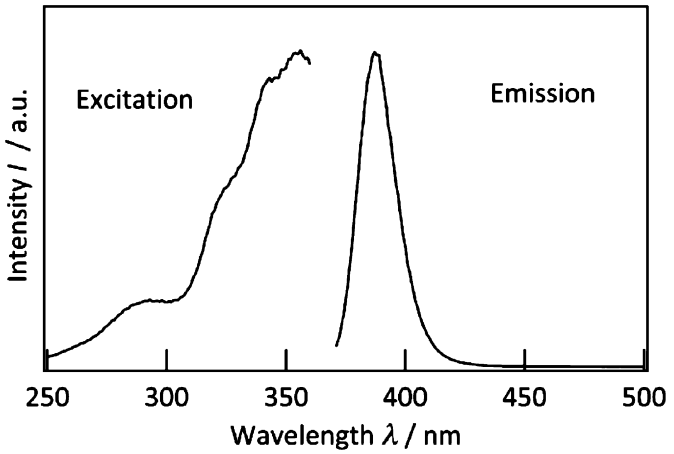

Fig. 8. Emission spectra of the luminescence of $NaZnAl(SO_4)_3$:0.01Eu^{2+}[30]. The spectra were recorded for 356 nm.

The center of gravity of the crystal-field splitting is affected by the host lattice anion. When the ligand anions share electrons with Eu^{2+} ion, the 5d level of Eu^{2+} shifts to lower energy. The ligand O^{2-} ions constitute the framework structure in the NASICON structure, and the bond character of the framework influences the nephelauxetic effect of O^{2-} on the 5d level of Eu^{2+} at the interstitial sites. For $A_{0.5}Zr_2(PO_4)_3$ (A = Ca, Sr, Ba), the $Zr_2(PO_4)_3$ framework was strictly covalent. Therefore, the nephelauxetic effect of O^{2-} did not change with the substitution of A ions because of the small changes in the $Zr_2(PO_4)_3$ framework. On the contrary, the nephelauxetic effect of O^{2-} is changed using a different NASICON framework. Recently, we investigated the luminescent properties of Eu-doped sulfate NASICON [30], $NaZnAl(SO_4)_3$:Eu^{2+}, which exhibited the Eu^{2+} emissions at higher energy than phosphate NASICONs (Fig. 8). As sulfur and aluminum have higher electronegativity (2.6 and 1.6) than phosphorus and zirconium (2.2 and 1.3) [31], the framework structure of the sulfate NASICON is more covalent than that of the phosphate. The nephelauxetic effect of O^{2-} in the sulfate NASICONs was smaller than the phosphate. This explains the shift to higher energy in the sulfate compared to the phosphates. A wide chromaticity of Eu^{2+} doped NASICONs is expected to be obtained by changing the cation and anion species in the framework structure.

4. Conclusion

Eu^{2+} doped NASICON structured $A_{0.5}Zr_2(PO_4)_3$ (A = Ca, Sr, Ba) phosphors exhibited the blue and blue-green colored emissions attributed to $4f^6 5d^1$–$4f^7$ transitions under UV excitation. Eu^{2+} ions located at two interstitial spaces in the $Zr_2(PO_4)_3$ framework, which consisted of covalent Zr–O and P–O bonds. The Eu–O bond length increased with the expansion of c axis from the Ca to Ba systems. The emission energies of Eu^{2+} ions were discussed on crystal field strength and the covalency of the framework structure. The Eu^{2+} emissions in the ionic environments shifted to higher energy with increasing Eu–O bond lengths due to the small crystal field splitting. The comparison to Eu^{2+}-doped sulfate NASICON indicated that, the framework composition changes center of gravity of the crystal-field splitting in Eu^{2+}. The two significant parameters vary with the elements forming the framework structure, making continuous control of the emissions from Eu^{2+} doped $A_{0.5}Zr_2(PO_4)_3$ phosphors.

References

[1] A. Zukauskas, M.S. Shur, R. Gaska, MRS Bull. 26 (2001) 764–769.
[2] Y. Narukawa, J. Narita, T. Sakaomto, T. Yamada, H. Narimatsu, M. Sano, T. Mukai, Phys. Status Solidi (a) 204 (2007) 2087–2093.
[3] X. Piao, K.I. Machida, T. Horikawa, H. Hanzawa, Y. Shimomura, N. Kijima, Chem. Mater. 19 (2007) 4592–4599.
[4] K. Uheda, N. Hirosaki, Y. Yamamoto, A. Naito, T. Nakajima, H. Yamamoto, Electrochem. Solid State Lett. 9 (2006) H22–H25.
[5] M. Hirayama, N. Sonoyama, A. Yamada, R. Kanno, J. Lumin. 128 (2008) 1819–1825.
[6] J.K. Sheu, S.J. Chang, C.H. Kuo, Y.K. Su, L.W. Wu, Y.C. Lin, W.C. Lai, J.M. Tsai, G.C. Chi, R.K. Wu, IEEE Photonics Technol. Lett. 15 (2003) 18–20.
[7] K.Y. Jung, H.W. Lee, H.K. Jung, Chem. Mater. 18 (2006) 2249–2255.
[8] S. Okamoto, H. Yamamoto, Electrochem. Solid State Lett. 10 (2007) J139–J142.
[9] P. Dorenbos, J. Lumin. 111 (2005) 89–104.
[10] H.Y.-P. Hong, Mater. Res. Bull. 11 (1976) 173–182.
[11] H. Fakrane, M. Lamire, A. El Jazouli, G. Le Flem, R. Olazcuaga, Ann. Chim. (Paris) 23 (1998) 77–80.
[12] K. Bakhous, F. Cherkaoui, A. Benabad, J.M. Savariault, Mater. Res. Bull. 34 (1999) 263–269.
[13] A. Meijerink, G. Blasse, J. Lumin. 43 (1989) 283–289.
[14] P. Dorenbos, J. Lumin. 104 (2003) 239–260.
[15] P. Dorenbos, J. Alloys Comp. 341 (2002) 156–159.
[16] J.S. Kim, P.E. Jeon, J.C. Choi, H.L. Park, Solid State Commun. 133 (2005) 187–190.
[17] J.B. Goodenough, H.Y.-P. Hong, J. Kafalas, Mater. Res. Bull. 11 (1976) 203–220.
[18] J. Alamo, R. Roy, J. Am. Ceram. Soc. 5 (1984) C-78.
[19] R. Roy, D.K. Agrawal, J. Alamo, R.A. Roy, Mater. Res. Bull. 19 (1984) 471–477.
[20] T. Masui, K. Koyabu, S. Tamura, N. Imanaka, J. Alloys Compd. 418 (2006) 73–76.
[21] A.I. Orlova, V.I. Pet'kov, O.V. Egor'kova, Radiochemistry 38 (1996) 13–19.
[22] F. Izumi, T. Ikeda, Mater. Sci. Forum 198 (2000) 321–324.
[23] W. Fischer, L. Singheiser, Powder Diffraction 19 (2004) 153–156.

[24] E.R. Gobechiya, Yu.K. Kabalov, V.I. Pet'kov, M.V. Sukhanov, Crystallogr. Rep. 49 (2004) 741–746.
[25] S. Thongchant, S. Katagiri, Y. Hasegawa, Y. Wada, S. Watase, M. Nakamoto, T. Sakata, H. Mori, S. Yanagida, Bull. Chem. Soc. Jpn. 77 (2004) 807–812.
[26] V.A. Pelova, L.S. Grigorov, J. Lumin. 72-4 (1997) 241–243.
[27] M. Buijs, A. Meyerink, G. Blasse, J. Lumin. 37 (1987) 9–20.
[28] V.I. Pet'kov, V.S. Kurazhkovskaya, A.I. Orlova, M.L. Spiridonova, Crystallogr. Rep. 47 (2002) 736–743.
[29] R.D. Shannon, Acta Crystallogr. Sect. A 32 (1976) 751–767.
[30] M. Hirayama, N. Sonoyama, A. Yamada, R. Kanno, submitted for publication
[31] L. Pauling, The Nature of the Chemical Bond, third ed., Cornell University Press, Ithaca, NY, 1960.